MODELING THE HEAT TRANSFER IN FLOW IN COMPLEX CHANNELS BY THE FINITE-ELEMENT METHOD

A. A. Mikhalevich and V. I. Nikolaev

UDC 536.24:532.54

The flow and heat transfer in closed and open channels are considered. The thermal part is solved in a conjugate formulation. In the numerical realization, tetragons are used, as well as automatic region generation and graphical packets for postprocessor analysis of the results.

Introduction

As is known, modeling velocity, temperature, and concentration fields in channels of complex form requires the solution of transport equations of Navier–Stokes type. As a rule, such flows are two- or three-dimensional, and include initial-section effects, recirculation zones, combined influence of natural and induced convection (taking account of buoyancy forces), etc.

In the last twenty years, there has been rapid development both of the mathematical models describing complex flows and heat transfer and of the computer base for the solution of such models. It is well known that the effective solution of hydrodynamic and thermal problems based on the complete Navier–Stokes equations (even with large Reynolds numbers) requires the use of superpowerful computers (productivity of the order of 10^9 flops) and is prohibitively expensive. However, the idea of reliable computer simulation of complex thermohydraulic processes is so fruitful that its supporters grow in number in proportion to the degree of computerizaton of scientific research.

1. Model of Turbulence

Although the Navier–Stokes equations themselves are sufficiently difficult to solve, in many practical cases the main complexity arises in the closure of a particular model of turbulence. As well as conceptual difficulties, there are purely mathematical complexities: the initial equations become nonlinear in this case, and have a small parameter in the largest derivative.

Most practical models of turbulence are based on the concept of vortex or turbulent viscosity and diffusion. The well-known gradient dependence between the pulsational and mean flow was determined by Boussinesq. Using the traditional notation, tensor symbolism, and the concept of Reynolds stress, this relation may be written in the form

$$-\overline{u_i' u_j'} = \nu_t \left(\frac{\partial \overline{U}_i}{\partial x_j} + \frac{\partial \overline{U}_j}{\partial x_i} \right) - \frac{2}{3} k \delta_{ij}. \qquad (1)$$

The mixing-path hypothesis for determining ν_t in Eq. (1) has distinguished itself in many practical cases. The popularity of this model results from its simplicity of use and its great practical range of applicability. Note, however, that vortex viscosity vanishes everywhere that the velocity gradient is zero, and this is far from reality. In addition, this model takes no account at all of the conductive transport of turbulence downstream (for example, there is a generator of vortices which are then entrained downstream by the mean flow). This model takes account of the generation of turbulence by the wall and its subsequent transport to the center of the channel. In addition to the fundamental impossibility of taking account of the transport of turbulence by convention and diffusion, purely "technical" difficulties arise in specifying the distribution of mixing lengths in channels of complex cross section. Admittedly, these difficulties may be somewhat reduced by using a modification of the model known as the Buleev model [1]. The characteristic dimension of turbulent transfer in this case is defined as

Institute of Nuclear Power, Academy of Sciences of the Belorussian SSR, Minsk. Translated from Inzhenerno-Fizicheskii Zhurnal, Vol. 59, No. 3, pp. 470-478, September, 1990. Original article submitted February 1, 1990.

0022-0841/90/5903-1171$12.50

$$\frac{1}{L}=\frac{1}{2\pi}\int_0^{2\pi}\frac{1}{l}\,d\omega, \tag{2}$$

where ℓ is the distance from the point to the channel wall in the direction ω. Equation (2) defines L with induced flow in closed channels. In the case of more complex flow (submerged jets, etc.), the scale of turbulence is approximated by a more complex dependence. Simplified expressions for the turbulent viscosity and the thermal diffusivity in the Buleev model are written in the form

$$\mu/\mu_{\text{т}}=0.2\,f_0(\eta)\,f_1(\eta)\,\gamma^*; \tag{3}$$

$$a/a_{\text{т}}=0.2\,f_0(\lambda\eta)\,f_1(\lambda\eta)\,\gamma^*; \tag{4}$$

$$f_0(\eta)=\exp(-\eta); \tag{5}$$

$$f_1(\eta)=[1-\exp(-\eta)]/\eta; \tag{6}$$

$$\eta=65/\gamma^*; \tag{7}$$

$$\lambda=\begin{cases}0.8+0.2/\mathrm{Pr}^{0.67}, & \mathrm{Pr}\leqslant 1, \\ 1.0, & \mathrm{Pr}>1;\end{cases} \tag{8}$$

$$\tag{9}$$

$$\gamma^*=\frac{L^2}{\nu}\left|\frac{\partial\overline{U}}{\partial n}\right|. \tag{10}$$

This model may be used for the integration of transport equations in the channel formed by a triangular bundle of longitudinally ribbed heat-exchanger tubes, in which a chemically reacting gas is used as the heat carrier. Below, the results of these calculations are outlined, and the specifics of heat and mass transfer in the presence of exo- and endothermal reactions are considered.

The deficiencies of the mixing-length hypothesis may be overcome in models based on the solution of transport equations for the turbulence characteristics. Models for the transport of the turbulence scale, defined as $\sqrt{k}$, where $k=\overline{u_iu_j}/2$, were the first to appear. In this case, it is important that the turbulence scale is determined without using the concept of a gradient relation between the velocity pulsations and the mean flow velocity directly from the transport equation. The Kolmogorov–Prandtl expression in this case takes the form

$$\nu_t=c_\mu\sqrt{k}\,L, \tag{11}$$

where c_μ is an empirical constant.

The accurate transport equation for the kinetic energy may be obtained from the Navier–Stokes equations. For large Reynolds numbers, they take the form [2]

$$\frac{\partial k}{\partial t}+\overline{U_i}\overset{\text{conv.}}{\frac{\partial k}{\partial x_i}}=\overset{\text{dif.}}{\frac{\partial}{\partial x_i}\left[u_i'\left(\frac{u_i'u_j'}{2}+\frac{P}{\rho}\right)\right]}- \tag{12}$$

$$-\overset{\text{gen.}}{u_i'u_j'\frac{\partial\overline{U_i}}{\partial x_j}}-\overset{\text{flot.}}{\beta g_i\overline{u_i'J}}-\overset{\text{dissip.}}{\nu\frac{\partial u_i'}{\partial x_j}\frac{\partial u_j'}{\partial x_i}}.$$

The total derivative of the kinetic energy is formed on account of: convection of the mean motion (conv.), turbulent diffusion of the velocity and pressure pulsations (dif.), generation in the interaction of the Reynolds stress with the mean-velocity gradients (gen.), and dissipation of the kinetic energy as thermal energy on account of viscous forces (dissip.). The flotational (flot.) term takes account of the interaction and mutual conversion of the kinetic energy of turbulence to potential energy on account of Archimedes forces.

Model relations for the terms on the right-hand side must be included in Eq. (12). Using the traditional gradient representation for the diffusional term and the Archimedes forces and the Kolmogorov concept for the approximation of the dissipative term, the k-th equation may be written in the form

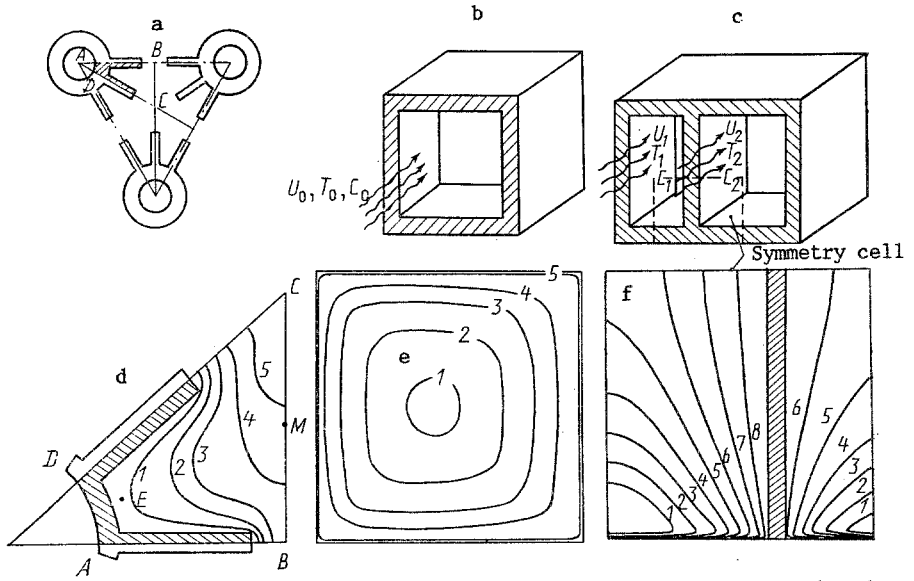

Fig. 1. Types of channels and corresponding flow diagrams (a-c); velocity isolines $\bar{U}$, m/sec, in ribbed tube bundle (d), with $\bar{U} = 0.1\bar{U}_{in}$ (1), $0.5\bar{U}_{in}$ (2), $\bar{U}_{in}$ (3), $1.8\bar{U}_{in}$ (4), and $2\bar{U}_{in}$ (5); in a rectangular channel, $v_0 = 0.5$ m/sec, $z/d_e = 0.4$ m (e), with $U = 0.83U_{in}$ (1) with $0.56U_{in}$ (2), $0.52U_{in}$ (3), $0.47U_{in}$ (4) and $0.18\bar{U}_{in}$ (5); and in an element of a plate heat exchanger (f), with $\bar{U} = 0.91\bar{U}_{in}$ (1), $1.83\bar{U}_{in}$ (2), $2.74\bar{U}_{in}$ (3), $3.65\bar{U}_{in}$ (4), $4.57\bar{U}_{in}$ (5), $5.48\bar{U}_{in}$ (6), $6.39\bar{U}_{in}$ (7), and $7.31\bar{U}_{in}$ (8).

$$\frac{\partial k}{\partial t} + \overline{U_i}\frac{\partial k}{\partial x_i} = \frac{\partial}{\partial x_i}\left(\frac{\nu_t}{\sigma_k}\frac{\partial k}{\partial x_i}\right) + \nu_t\left(\frac{\partial \overline{U_i}}{\partial x_j} + \frac{\partial \overline{U_j}}{\partial x_i}\right)\frac{\partial \overline{U_i}}{\partial x_j} + \\ + \beta g_i \frac{\nu_t}{\sigma_t}\frac{\partial \Phi}{\partial x_i} - c_d\frac{k^{3/2}}{L}. \tag{13}$$

The empirical quantities $\sigma_k = 1$ and $c_\mu c_d \approx 0.08$ in this relation are used in many energetic models in various works.

A significant deficiency of the given k model is that the linear dimension (scale) of the turbulence L appears in the last formula. In some cases, it may be determined by means of simple empirical dependences of the type of the Karman formula. In other cases, the dependences are more complex, for example those in [1, 2].

As is evident from the k-th equation itself, the model with one equation even allows (in contrast to the Prandtl equation) the convection and diffusional transport and the previous history of the process to be taken into account. However, its applicability is still limited by the relatively simple shear flows for which it is possible to determine L. These difficulties may be avoided in the model in which the scale of turbulence (or, equivalently, the dimensions of the large energy-containing vortices) is described by the transport equation. Most commonly, the equation is not written for the scale L itself, but for the combination $\varepsilon \approx k^{3/2}L$, which is known as the dissipation rate of the kinetic energy of turbulence.

The transport equation for the transport of ε is obtained from the Navier–Stokes equations, and takes the following form for the case of large Re (taking account of the model assumptions regarding the diffusion, generation, and dissipation terms appearing there)

$$\frac{D\varepsilon}{\partial t} = \frac{\partial}{\partial x_i}\left(\nu_t\frac{\partial \varepsilon}{\partial x_i}\right) + c_1\frac{\varepsilon}{k}\nu_t\left(\frac{\partial \overline{U_i}}{\partial x_j} + \frac{\partial \overline{U_j}}{\partial x_i}\right)\frac{\partial \overline{U_i}}{\partial x_j} - c_2\frac{\varepsilon^2}{k}\rho. \tag{14}$$

To determine the vortex viscosity, the Kolmogorov formula is used

$$\nu_t = c_\mu\frac{k^2}{\varepsilon}, \tag{15}$$

and the constants in Eqs. (13) and (14) are usually taken from [3], since they are based on extensive material regarding free shear flow ($c_\mu = 0.09$, $c_1 = 1.44$, $c_2 = 1.92$; $\sigma_k = 1.0$, $\sigma_\varepsilon = 1.3$). Equations (13) and (14) are used for many flows, although it must be noted that they are not universal. For some cases, other values of the empirical constants are used. The region of applicability of the k–ε model is expanded if the corresponding functions of the flow parameters are introduced instead of the constants. The energetic models of k–ε type are perhaps the most popular in calculating recirculational flow (where it is difficult to obtain the distribution of the linear turbulence scales). Adding algebraic relations (to take account of the buoyancy forces and other factors), the range of applicability of k–ε models may be much expanded.

The present work does not undertake the description of more complex models, since the authors have not had occasion to make use of them. It will simply be noted that models of turbulence based on equations of Reynolds-stress transport are sufficiently complex in realization and expensive in operation. Therefore, such models, despite their great potential, are very rarely used in practice.

All the foregoing applies to the modeling of large vortices using closed models for supergrid scales (large-scale turbulence). The complete Navier–Stokes equations have only been solved for the simplest cases (laminar flows at small Re) in the last 100 years, and further progress in this direction will be determined by the increase in computer power.

2. Parabolic Flow in Closed Channels. Initial Equations

The flow diagram and the types of channels considered are shown in Fig. 1. To describe the hydrodynamic part of the problem, the model of parabolic flow is employed. In this case, consideration is confined to flow with no buoyancy forces (pressure-head flow) and only the longitudinal component of the velocity vector is taken into account (this is correct in rectilinear channels of constant cross secton at large Reynolds numbers). The model contains all the assumptions associated with a Newtonian liquid. The system of transport equations is based on continuity, motion, energy, diffusion, and heat-conduction equations. The numerical realizaton is based on the finite-element method.

The initial system of equations is

$$\rho\bar{U}_3\frac{\partial\bar{U}_3}{\partial x_3} = -\frac{\partial\bar{P}}{\partial x_3} + \frac{\partial}{\partial x_1}\left[(\mu+\mu_T)\frac{\partial\bar{U}_3}{\partial x_1}\right] + \frac{\partial}{\partial x_2}\left[(\mu+\mu_T)\frac{\partial\bar{U}_3}{\partial x_2}\right]; \tag{16}$$

$$\rho c_p\bar{U}_3\frac{\partial\bar{T}}{\partial x_3} = \frac{\partial}{\partial x_1}\left[(\lambda+\lambda_T)\frac{\partial\bar{T}}{\partial x_1}\right] + \frac{\partial}{\partial x_2}\left[(\lambda+\lambda_T)\frac{\partial\bar{T}}{\partial x_2}\right] + S_T; \tag{17}$$

$$\rho\bar{U}_3\frac{\partial\bar{C}_k}{\partial x_3} = \frac{\partial}{\partial x_1}\left[\rho(D+D_T)\frac{\partial\bar{C}_k}{\partial x_1}\right] + \frac{\partial}{\partial x_2}\left[\rho(D+D_T)\frac{\partial\bar{C}_k}{\partial x_2}\right] + R_k. \tag{18}$$

The continuity equation is expediently used in integral form

$$\int_S \rho\bar{U}_3 ds = \text{const}, \tag{19}$$

where S is the cross section of the channel. The heat-conduction equation in the ribbed wall is added to the system in Eqs. (16)-(19)

$$\frac{\partial^2\bar{T}}{\partial x_1^2} + \frac{\partial^2\bar{T}}{\partial x_2^2} = 0. \tag{20}$$

The pressure variation – the source term in Eq. (16) – is found from the condition of conservation of the mass flow rate through the channel cross section. The turbulent-transfer coefficients used in Eqs. (16)-(20) are calculated from the Buleev model. The turbulent diffusion coefficients are determined from the relation

$$D/D_T = \text{Pr}_D(\mu/\mu_T). \tag{21}$$

The specific feature of the given problem is that exothermal and endothermal reactions occur in the heat carrier. A chemically reacting gas consisting of several components is considered. Change in composition of the heat carrier occurs here. The concentration distribution of the

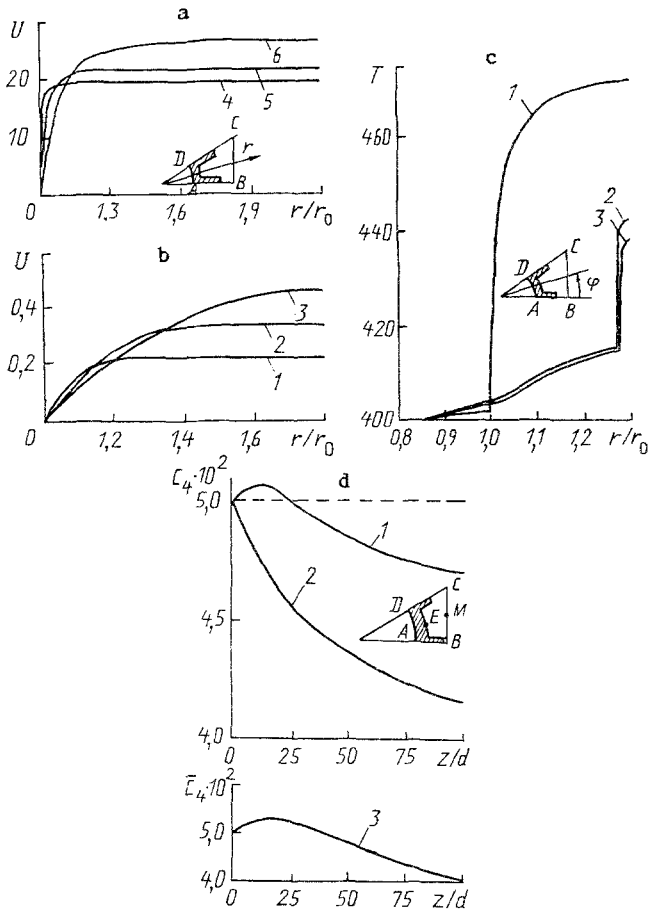

Fig. 2. Distribution of velocity (m/sec) along the radius in turbulent (a) and laminar (b) flow in a ribbed bundle, with z/d_e = 0.25 (1), 1.0 (2), 3.0 (3), 10.0 (4), 30.0 (5), and 70.0 (6); temperature distribution, K, along the radius for the same bundle (c) with φ = 15° (1), 3° (2), and 0 (3); distribution of C_4 (oxygen) (d) at characteristic points of the channel: 1) M; 2) E; 3) mean mass value $\bar{C}_4$.

heat-carrier components is described by the convective-diffusion Eq. (18). In view of the complexity and unwieldiness of the calculations and procedures for determining the coefficients μ, λ, c_p, and D of chemically reacting gas, these expressions are not given here, and neither are the algorithms and specifics of the calculation of the source terms S_m and R_k in Eqs. (17) and (18), on the assumption that this issue is not fundamental to the solution of the initial system. This material may be found in [4].

Boundary Conditions and Method of Calculation. To obtain the results given below, simultaneous solution of four partial differential equations describing the three-dimensional (for the longitudinal velocity) flow and heat and mass transfer of chemically reacting gas is required. The channel cross section is sufficiently complex in form. The given problem is far from trivial, and requires the applicaton of an effective numerical method for its solution. The finite-element method is used in the Galerkin modification (method of weighted discrepancies) [5]. The basis functions adopted are functions of the Langrangian family for isoparametric linear of quadratic tetragons. Integration of the initial equations in the downstream direction is by means of a two-layer purely implict scheme. The NIKABT program has been widely used and tested, without any significant problems associated with the convergence or stability of the solution, although it must be noted that oscillations of the numerical values in the computation process may be found. Simultaneous reduction in size of the element and in the longitudinal integration step significantly reduces the scale of the oscillations.

Solution requires the specification of boundary values at all the boundaries of the integration region and values of the given functions at the channel input, where plane pro-

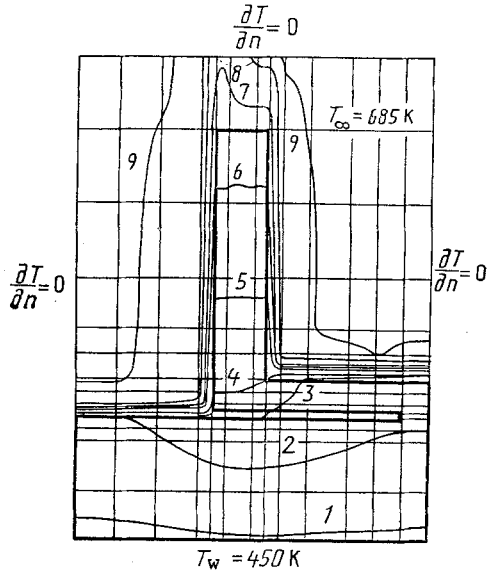

Fig. 3. Isotherms in a heat-exchanger element (ribbed wall, gas flow): 1) 480; 2) 490; 3) 520; 4) 540; 5) 590; 6) 620; 7) 640; 8) 670; 9) 680 K.

files of all the functions ($\bar{U}_{in}$, $\bar{T}_{in}$, $\bar{C}_{kin}$) are specified. Neumann conditions are specified at the symmetry lines, and at the thermally loaded boundary of the region provision is made for the use of heat-transfer boundary conditions of the first, second, and third kinds, as well as any combination of these. At the gas–wall heat-transfer surface, conditions of thermal matching of the temperatures and the normal components of the heat fluxes are satisfied.

The mathematical model and packet of programs used in the present work may be successfully applied to the description and modeling of a broad class of so-called parabolic flows in closed channels of complex form. Some results of numerical experiments are given below, with details associated with their conduct. Isolines of the given functions in a rectangular channel, a system of two parallel heat-exchanger channels, and a channel formed by a triangular bundle of longitudinally ribbed tubes are shown in Fig. 1. All these channels are elements of heat exchangers of various types (shell-and-tube heat exchangers with smooth and ribbed tube bundles and plate heat exchangers). The position of the isolines permits judgments regarding the nonuniformity of the velocity and temperature profiles and the observation of zones of greatest gradient and stagnant zones in the channels.

In the case of laminar flow in a ribbed bundle of tubes (Fig. 2a, b), the velocity profiles are less steep than in turbulent conditions, of course. The presence of ribbing leads to strong angular nonuniformity of the velocity in the initial section which, in turn, has a significant influence on the formation of temperature and concentration fields in the flow.

The intersection of the curves in Fig. 2c indicates the redistribution of heat fluxes in the ribbed wall of the tube.

Variation in oxygen concentration and the local temperature at characteristic points of the channel occurs in different ways (Fig. 2d). There are characteristic surges due to the specifics of the chemical reactions in the heat carrier.

In modeling a rectangular channel, flow in a square channel with different thermal conditions at the external surface is considered. The local velocity, temperature, and concentration values in the channel cross sections are calculated [6].

The conjugate temperature field in the ribbed wall is shown in Fig. 3. The distinguishing feature of this case is that the surface ribbing is by means of welded U-shaped grooves, and the influence of the contact resistance and the gap on the formation of the temperature profile in this structure is investigated.

One of the most interesting examples realizing the possibility of direct numerical modeling and the finite-element method, in our view, is the calculation of the flow and heat transfer in elements of plate heat exchangers [6]. This is essentially a thermohydraulic calculation of an elementary heat exchanger based on the solution of the basic transport conservation equations. As well as the calculation of the local temperature and velocity values (velocity isolines are shown in Fig. 1), the distribution of local Nu values along the cold and hot sides of the dividing wall is obtained [6].

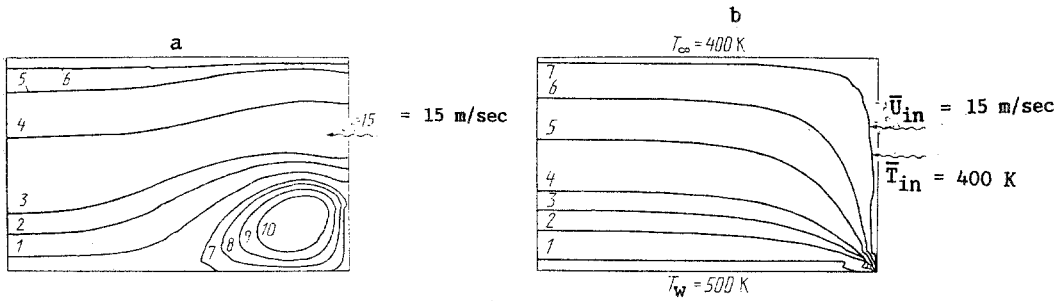

Fig. 4. Streamlines ψ (a) and isotherms T (b) in transverse flow around an inverse projection: a) ψ = −0.04 m²/sec (1), 0.1 (2), 0.16 (3), 0.4 (4), 0.48 (5), −0.54 (6), 0.012 (7), 0.04 (8), 0.06 (9), 0.09 (10); b) T = 499 K (1), 485 (2), 470 (3), 460 (4), 440 (5), 420 (6), 403 (7).

3. Elliptical Flow (Flow around a Projection). Initial Equations

To describe the recirculational flow arising behind a projection and the heat transfer between the flow and the ribbed wall in the flow, the following system of equations must be solved:

$$\rho\bar{U}_j\frac{\partial\bar{U}_i}{\partial x_j}=-\frac{\partial\bar{P}}{\partial x_i}+\frac{\partial}{\partial x_j}\left(\mu\frac{\partial\bar{U}_i}{\partial x_j}-\overline{\rho u_i'u_j'}\right); \tag{22}$$

$$\frac{\partial(\rho\bar{U}_i)}{\partial x_i}=0; \tag{23}$$

$$\rho\bar{U}_j\frac{\partial\bar{T}}{\partial x_i}=\frac{\partial}{\partial x_j}\left(\frac{\mu}{\mathrm{Pr}}\frac{\partial\bar{T}}{\partial x_j}-\overline{\rho u_i'T}\right); \tag{24}$$

$$\rho\bar{U}_j\frac{\partial k}{\partial x_j}=\frac{\partial}{\partial x_j}\left(\frac{\mu_T}{\sigma_k}\frac{\partial k}{\partial x_j}\right)-\overline{\rho u_i'u_j'}\frac{\partial\bar{U}_j}{\partial x_j}-\rho\varepsilon; \tag{25}$$

$$\rho\bar{U}_j\frac{\partial\varepsilon}{\partial x_j}=\frac{\partial}{\partial x_j}\left(\frac{\mu_T}{\sigma_\varepsilon}\frac{\partial\varepsilon}{\partial x_j}\right)-C_1\frac{\varepsilon}{k}\overline{\rho u_i'u_j'}\frac{\partial\bar{U}_i}{\partial x_j}-c_2\rho\frac{\varepsilon^2}{k}. \tag{26}$$

To determine the vortex viscosity, Eq. (15) is added to the system, and in place of the continuity equation in Eq. (23) the Poisson equation for the pressure may be solved; this equation is obtained from the Navier–Stokes equations by cross differentiation of the equations for the velocity components $\bar{U}_i$ and $\bar{U}_j$

$$\nabla^2\bar{P}=\frac{\partial}{\partial x_i}\left[-\bar{U}_j\left(\frac{\partial\bar{U}_i}{\partial x_j}-\frac{\partial\bar{U}_j}{\partial x_i}\right)\right]+\frac{\partial}{\partial x_j}(2\nu_T\bar{S}_{ij}), \tag{27}$$

where

$$S_{ij}=\frac{1}{2}\left(\frac{\partial\bar{U}_i}{\partial x_j}+\frac{\partial\bar{U}_j}{\partial x_i}\right). \tag{28}$$

Results and Discussion

The flow behind a projection is calculated using quadratic tetragons. The region is constructed using an automatic data-generation program, and the output digital information is processed by means of graphical packets. The characteristic pattern of streamlines behind a projection and the distribution of the temperature field in the given region are shown in Fig. 4.

Note, in conclusion, that the calculations are performed on an EC-1061 computer. The finite-element method, although it requires considerable working store of the computer (all the programs occupy around 2 Mbyte), is sufficiently effective, and permits the investigation of the most different forms of channels (annular, triangular, etc.) without considerable program modification.

The use of service programs for pre- and postprocessor analysis of the information permits the conversion of the program complex from the purely "scientific" to the "engineering"

level and its application as an elementary basis for the creaton of various types of automated-design systems.

NOTATION

$\bar{U}_i$, mean velocity in i-th direction; u_i', velocity pulsations in i-th direction; $\bar{C}_k$, mean concentration of k-th component; $\bar{T}$, mean temperature; ρ, density; c_p, specific heat at constant pressure; μ, viscosity of heat carrier; Pr, Prandtl number; Pr_D, diffusional Prandtl number; R_k, heat source (sink) on account of chemical reactions; d_e, equivalent diameter; S_T, mass source (sink) in chemical reaction; $\bar{P}$, mean pressure; n, vector normal; β, volume-expansion coefficient; k, kinetic energy of turbulence; ε, dissipation rate of kinetic energy of turbulence; ∇^2, Laplacian operator; I, pulsations of a scalar quantity; Φ, instantaneous or mean value of a scalar quantity.

LITERATURE CITED

1. N. I. Buleev, Heat Transfer [in Russian], Moscow (1962), pp. 64-98.
2. V. Rodi, Methods of Calculating Turbulent Flow [Russian translation], Moscow (1984), pp. 227-322.
3. B. E. Lounder and D. B. Spolding, Comp. Meth. Appl. Mech. Eng., No. 3, 269-280 (1974).
4. V. I. Nikolaev, V. A. Nemtsev, and L. N. Shegidevich, Vestsi AN BSSR, Ser. Fiz.-Énerg. Navuk, No. 1, 43-47 (1987).
5. O. Zenkevich, Finite-Element Method in Engineering [in Russian], Moscow (1975).
6. A. A. Mikhalevich, V. I. Nikolaev, and V. I. Fedosova, Inzh.-Fiz. Zh., 57, No. 2, 246-253 (1989).

DYNAMICS OF Z-PINCH WITH A LIGHT LINER.

1. DESCRIPTION OF THE MODEL AND CALCULATION OF DOUBLE-SHELL LINERS

G. S. Romanov, A. S. Smetannikov, Yu. A. Stankevich, and V. I. Tolkach

UDC 533.9

The compression of a plasma by a plastic liner has been modeled computationally in the one-dimensional magnetic radiation gasdynamic approximation. The dynamics of the process has been considered with allowance for the deviation from local thermodynamic equilibrium.

Intensive studies have been under way on the compression of a plasma by cylindrical shells (liners), driven toward the symmetry axis by the pressure of the intrinsic magnetic field. These studies have been stimulated by the potential extensive applications in obtaining plasmas with high parameters, producing ultrastrong pulsed magnetic fields, etc. High-power sources of short-wavelength radiation, arising as a result of thermalization of the kinetic energy when the liner "stops" at the axis, have been developed on this basis. Considerable progress in the studies has been made by using high-power nanosecond electrical generators as the power supply [1]. The generated current pulses of several megaamperes with a length of the order of 100 nsec allow the liner to be accelerated to velocities of several hundreds of kilometers per second (light liners with a mass of ~100 μg/cm and an initial radius of ~1 cm). These studies call for a detailed investigation of the physics of the processes, which is very difficult to carry out experimentally. Of particular interest in such problems is the efficiency with which energy from the power supply is converted to the kinetic energy of the linear and then to radiant energy. Moreover, by means of simple analytical solutions it is possible to consider only individual aspects of the compression.

Scientific-Research Institute of Applied Physical Problems, V. I. Lenin Belorussian State University, Minsk.

Translated from Inzhenerno-Fizicheskii Zhurnal, Vol. 59, No. 3, pp. 479-487, September, 1990. Original article submitted April 3, 1990.

0022-0841/90/5903-1178$12.50